Investigation of complexity dynamics in a DC glow discharge magnetized plasma using recurrence quantification analysis

Vramori Mitra, Bornali Sarma, Arun Sarma, M. S. Janaki, A. N. Sekar Iyengar, Norbert Marwan, and Jürgen Kurths

Articles you may be interested in

Investigation and quantification of nonlinearity using surrogate data in a glow discharge plasma
Phys. Plasmas **22**, 022307 (2015); 10.1063/1.4907796

Investigation of complexity dynamics of inverse and normal homoclinic bifurcation in a glow discharge plasma
Phys. Plasmas **21**, 032301 (2014); 10.1063/1.4867064

Study of nonlinear oscillations in a glow discharge plasma using empirical mode decomposition and Hilbert Huang transform
Phys. Plasmas **20**, 022301 (2013); 10.1063/1.4789853

Continuous wavelet transform based time-scale and multifractal analysis of the nonlinear oscillations in a hollow cathode glow discharge plasma
Phys. Plasmas **16**, 102307 (2009); 10.1063/1.3241694

Time series analysis of ionization waves in dc neon glow discharge
Phys. Plasmas **13**, 073504 (2006); 10.1063/1.2219420

Investigation of complexity dynamics in a DC glow discharge magnetized plasma using recurrence quantification analysis

Vramori Mitra,[1] Bornali Sarma,[1] Arun Sarma,[1] M. S. Janaki,[2] A. N. Sekar Iyengar,[2] Norbert Marwan,[3] and Jürgen Kurths[3,4]

[1]VIT University, Vandalur-Kelambakkam Road, Chennai 600 127, Tamil Nadu, India
[2]Plasma Physics Division, Saha Institute of Nuclear Physics, 1/AF, Bidhannagar, Kolkata 700064, India
[3]Potsdam Institute for Climate Impact Research, PO Box 601203, 14412 Potsdam, Germany
[4]Institute for Complex Systems and Mathematical Biology, University of Aberdeen, Aberdeen AB24 3FX, United Kingdom

Recurrence is an ubiquitous feature which provides deep insights into the dynamics of real dynamical systems. A suitable tool for investigating recurrences is recurrence quantification analysis (RQA). It allows, e.g., the detection of regime transitions with respect to varying control parameters. We investigate the complexity of different coexisting nonlinear dynamical regimes of the plasma floating potential fluctuations at different magnetic fields and discharge voltages by using recurrence quantification variables, in particular, *DET*, L_{max}, and *Entropy*. The recurrence analysis reveals that the predictability of the system strongly depends on discharge voltage. Furthermore, the persistent behaviour of the plasma time series is characterized by the Detrended fluctuation analysis technique to explore the complexity in terms of long range correlation. The enhancement of the discharge voltage at constant magnetic field increases the nonlinear correlations; hence, the complexity of the system decreases, which corroborates the RQA analysis. *Published by AIP Publishing.* [http://dx.doi.org/10.1063/1.4953903]

I. INTRODUCTION

Recurrence Quantification analysis (RQA) of nonlinear time series is a relatively new and advanced technique which helps to identify different dynamical regimes by giving both visual information and also several quantification variables. RQA is widely accepted for revealing the complexity and predictability of natural systems. The base of RQA is the recurrence plot (RP), introduced in 1987 by Eckman *et al.* as a simple mathematical tool for visualizing the recurrence behaviour of phase space trajectories.[1] RPs and RQA have been extensively used in diverse fields such as life science,[2] earth science,[3] plasma,[4,5] astrophysics,[6] and finance and economy[7] to gain understanding about the nonlinear dynamics of complex systems.[8] In fusion plasmas, turbulence and associated cross field transport have been investigated by using RQA.[9,10] It has also been utilized as an emerging tool to analyze simulation data of ion temperature gradient turbulence[11] and dissipative trapped electron mode turbulence,[12] and to characterize transport dynamics. Recently, we have used RQA to study order-chaos transition in an unmagnetized DC glow discharge plasma oscillation.[13] We have investigated the robustness of RQA variables in the presence of different noise levels. We have utilized the RP and RQA as an important tool for identifying the normal and inverse homoclinic bifurcation in a double plasma system near a plasma fireball.[14] The enhancement of the time period in the data obtained from both experiment and numerical modelling with respect to a controlling parameter is clearly observable in the RP. Weighted recurrence plot is an alternative for Shannon entropy to access the complexity of a dynamical system.[15] Entropy based quantifiers of RPs, e.g., the normalized entropy of recurrence times or the Shannon entropy, are

able to indicate points of bifurcation and it can be a valuable alternative to Lyapunov exponents as calculation of Lyapunov exponents is often difficult for systems whose equations of motion are unknown. Hence, RQA estimators can be used to efficiently describe the divergence behavior of the dynamical system.

There have been several experimental studies on plasma systems which reflect many interesting features such as self-excited oscillations, period doubling, intermittency, strange attractors, and other routes to chaos.[16–18] Like any other dynamical system, a plasma system exhibits transitions from one state to another when a specific control parameter is altered.[19–21] Qin *et al.*[22] reported about the period-doubling sequence and intermittency in an undriven steady-state plasma by experimental observations. Nurujjaman *et al.*[23] investigated nonlinear dynamical behaviour like the homoclinic bifurcation in the floating potential fluctuations at different discharge voltages in a cylindrical DC glow discharge plasma system by using the conventional nonlinear techniques like correlation dimension, largest Lyapunov exponent, etc.

In this report, an attempt has been made to introduce recurrence quantification analysis (RQA) and detrended fluctuation analysis (DFA) technique to explore and investigate the nonlinear dynamical behaviour and associated complexity of the glow discharge plasma oscillations in the presence of an external magnetic field. Various observations on periodic and quasi periodic oscillations and its analysis have been carried out in a magnetized glow discharge plasma system. The visual change in RPs determines the transitions of the floating potential fluctuations under variation of magnetic fields and discharge voltages. RQA mainly based on the point density and length of the diagonal and vertical line

23, 062312-1

structures in the RP is used to quantify the complexity of the floating potential fluctuations in different low magnetic fields and discharge voltages. The gradual change of the RQA measures due to different values of the controlling parameters quantitatively identifies the dynamical regimes of the plasma system. The investigation of long range correlation of the floating potential fluctuations has been performed by using DFA,[24] which is used to estimate the scaling behaviour of noisy data in the presence of different trends and determine the long range correlation of the time series.[25] The erratic fluctuations in plasma oscillations have been studied to extract robust features hidden in these complex fluctuations. DFA measures only one exponent of a signal which is helpful for studying mono fractal signals which have the same scaling properties.

The remainder of the paper is organized as follows: Section II gives the theoretical aspects of different analysis techniques. Section III describes the experimental setup, while in Section IV we report the results of the nonlinear analysis. Conclusions are drawn in Sec. V.

II. ANALYSIS TECHNIQUES

A. Power spectral analysis

Power spectral analysis is a novel tool having a wide range of applications in diverse fields. It gives the essence of understanding of energy variations as a function of frequency. It reflects at which frequencies variations (energy) are strong and at which frequencies variations are low. Spectral analysis is directly computed by using the fast Fourier transform (FFT) algorithm. FFT is a mathematical method for transforming a function of time into a function of frequency.

B. State space reconstruction

The reconstruction of the attractor gives a powerful impetus to investigate the natural phenomena in real systems. Embedding dimensions (d) are computed for each time series by using the false nearest neighbor method (FNN).[35] The embedding dimension has been selected when the number of false nearest neighbors approaches zero. Time delays τ are calculated from the first minimum of the average mutual information function.

C. Recurrence plot and recurrence quantification

In the analysis of dynamical systems, it is essential to observe the state of a system in phase space. The recurrence plot was introduced to visualise system's state evolution in the reconstructed phase space. According to Taken's embedding theorem,[26] using a time series data X_i an embedding can be made using the vector $\vec{Y}_i = \vec{X}_i; \vec{X}_{i+\tau}; \vec{X}_{i+(d-1)\tau}$, where d is the embedding dimension and τ is the time delay. The false nearest neighbor and mutual information method estimates the correct embedding parameters which preserve the topological properties of the phase space.[27] The original time series is now embedded into a d-dimensional reconstructed phase space. A recurrence is said to occur whenever a trajectory visits approximately the same region of phase space. The RP is formally defined by the square matrix

$$R_{i,j} = H(\epsilon - ||\vec{Y}_i - \vec{Y}_j||), \quad i,j = 1, 2, ...N,$$

where ϵ is a predetermined threshold, H is the Heaviside unit step function, and N is the number of data points of the signal. Both the axes of the graph represent the temporal extent to which the signal spans. The RP is obtained by plotting the recurrence matrix using different colors (white and black) for its binary entries.

The visual inspection of RP reveals some small scale structures such as single dots, diagonal, vertical, and horizontal lines. Diagonal lines in the plots are indicative of deterministic behaviour and indicate similar evolution of states at different times.[28] States that change slowly, like those occurring during laminar phases cause horizontal and vertical lines. Dynamical states can cause single isolated points if the states are rare, persistence is less or if they fluctuate heavily.[29] Several statistical measures have been introduced to quantify the small scale structures appearing in the RP which form a diagnostic tool known as recurrence quantification analysis (RQA).[30–32]

As already stated, diagonal lines represent to different segments of the phase space trajectory that evolve very close and in parallel. These lines are therefore related to the divergence properties of the dynamics and, thus, determinism and predictability. The RQA measure *determinism (DET)* is quantifying these characteristics. It is the fraction of recurrence points that form diagonal lines

$$DET = \frac{\sum_{l=l_{min}}^{N} lP(l)}{\sum_{l=1}^{N} lP(l)},$$

where $P(l)$ is the histogram of the diagonal lines of length l. When a system is periodic, a RP shows non interrupted diagonal lines and DET becomes close to unity. DET approaches zero when the behaviour is random as recurrence points are mainly arranged by single dots and not as diagonal lines. Further RQA measures related to diagonal lines are average diagonal line length or Shannon entropy of the line length distribution (*ENT*). *ENT* indicates the Shannon entropy of the probability

$$p(l) = P(l)/N_l,$$

to find a diagonal line of exactly length of l in the RP. It is estimated by

$$ENT = -\sum_{l=l_{min}}^{N} p(l)lnp(l).$$

The variable entropy reflects the complexity of the oscillation through the distribution of the diagonal line. The inverse of the longest diagonal line (L_{max}) in the RP is indirectly related to the largest Lyapunov exponent via its relationship to the Renyi entropy of second order. It is defined by

$$L_{max} = max((l_i)_{i=1}^{N_l}),$$

small values of L_{max} elucidate more chaotic or complex dynamics of the system.

D. Detrended fluctuation analysis

Detrended fluctuation analysis (DFA) is a method, developed to explore the scaling behaviour of fractal and multifractal non-stationary time series. DFA is widely used in diverse fields of interest as medical science,[40–44] economical time series,[45,46] climate research,[47,48] and solid state physics[49,50] to determine the long range persistent behaviour of physical and biological complex dynamical systems. Plasma fluctuations reflect multifractal, scale invariant features, characterised by long range power law correlations. We have elucidated the fractal properties and correlation properties of time series of plasma oscillations obtained in various experimental conditions by using the DFA method. DFA consists of the following steps. In the first step, the mean of the signal $s(i)$ is subtracted from the signal and then integrated, where $i = 1, 2, \ldots N$ and N is the length of the signal. It is expressed as

$$y(i) = \sum_{j=1}^{i} [s(j) - \bar{s}],$$

where $\bar{s}$ stands for the mean. The profile $y(i)$ is then divided into segments of equal length n. Each segment $y(i)$ is fitted by using a polynomial function $y_n(i)$, which shows the local trend in the box. Next the profile is detrended by removing the local trend represented as

$$Y_n = y(i) - y_n(i).$$

Finally, the root mean square (rms) fluctuation function is estimated by

$$F(n) = \sqrt{\frac{1}{n} \sum_{i-1}^{N} [Y_n(i)]^2}.$$

The scaling behaviour of $F(n)$ over a broad number of scales is obtained by repeating the above calculation for varied box length n

$$F(n) \propto n^{\alpha},$$

where α is the scaling exponent, named as Hurst exponent(H).

III. EXPERIMENTAL SETUP

The complete set of experiments have been carried out in a glow discharge plasma system having a stain less steel made chamber of length 50 cm and diameter 20 cm.[33] The schematic diagram of the experimental set up is shown in Fig. 1. A rotary pump is used to evacuate the system up to base pressure 0.001 mbar, and the pressure inside the chamber has been controlled by a needle valve. Argon (Ar) plasma is produced inside the system at required working pressure by applying a voltage between anode and cathode. For the creation of a magnetic field a Helmholtz coil is

wound over the cylindrical vessel and a DC current is passed through the coil. The Langmuir probe of diameter 2 mm is placed in the middle of the device for measuring the floating potential fluctuations (V_f). The electron density and temperature measured by the Langmuir probe are of the order of 10^{12}cm^{-3} and 2–6 eV, respectively. The time series corresponding to the floating potential fluctuations data are collected in the oscilloscope, and further, various nonlinear and statistical analyses are carried out with the help of recurrence quantification analysis and detrended fluctuation analysis (DFA) technique to evaluate their dynamical and statistical behaviour.

IV. RESULTS AND ANALYSIS

The experiment is carried out in 0.4 mbar pressure and 9 G, 28 G, and 46 G magnetic fields. The discharge voltage is varied from 408 V to 655 V, respectively, in corresponding magnetic fields. The magnetic field and the discharge voltage are considered as controlling parameters of the experiment. The dynamics of the plasma oscillations are sensitive on the controlling parameter and with the variation of the controlling parameters, it shows periodic, quasi periodic, chaotic, and relaxation oscillations. At 9 G magnetic field, the discharge struck at 408 V. The discharge voltage is varied for different magnetic fields. Figs. 2–4 shows the time series of floating potential fluctuation (V_f) (a$_1$–f$_1$), power spectra (a$_2$–f$_2$), and state space plot (a$_3$–f$_3$) with the increase in the discharge voltages in the presence of 9 G, 28 G, and 46 G external magnetic fields.

Figs. 2(a$_1$)–2(f$_1$) and 3(a$_2$)–3(f$_2$) show that in 9 G and 28 G magnetic fields, plasma oscillations are exhibiting periodic and quasi periodic behavior. The oscillations become chaotic around 597 V in a 46 G magnetic field as shown in Fig. 4 with the chaotic phase disappearing at about 603 V, leading to the relaxation oscillation of increasing time period.

A. Power spectral analysis

Power spectral analysis of the raw data is carried out and shown in Figs. 2(a$_2$)–2(f$_2$), 3(a$_2$)–3(f$_2$), and 4(a$_2$)–4(f$_2$). In Fig. 2(a$_2$), most of the frequencies are concentrated below 100 kHz and the dominant mode is observed at 49 kHz. With a further increase in discharge voltage, the dominant peak is
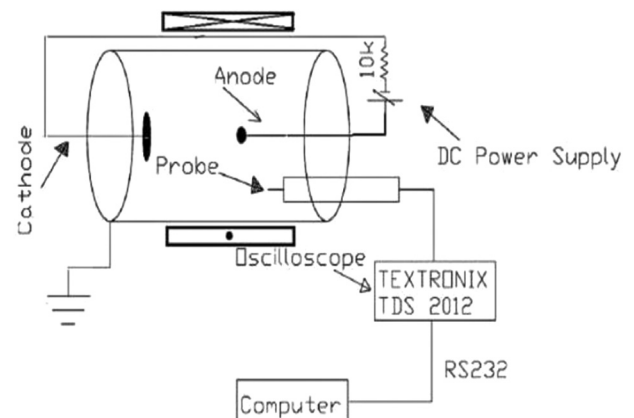

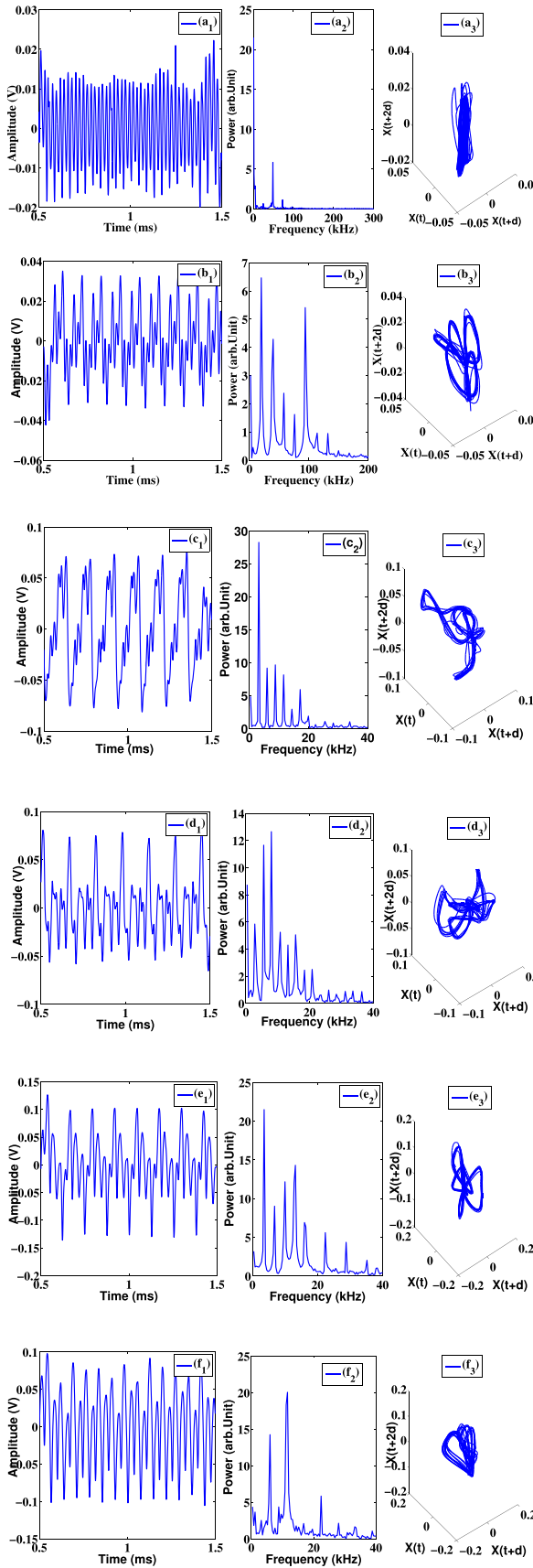FIG. 1. Schematic diagram of the whole experimental setup.

FIG. 2. (a$_1$)–(f$_1$) time series of floating potential fluctuations (V_f) at different values of discharge voltages: (a) 408 V, (b) 423 V, (c) 471 V, (d) 499 V, (e) 558 V, and (f) 569 V in 9 G magnetic field; (a$_2$)–(f$_2$) different values of power spectra of the corresponding signal; (a$_3$)–(f$_3$) 3D reconstructed states space of V_f for the same values of discharge voltages.
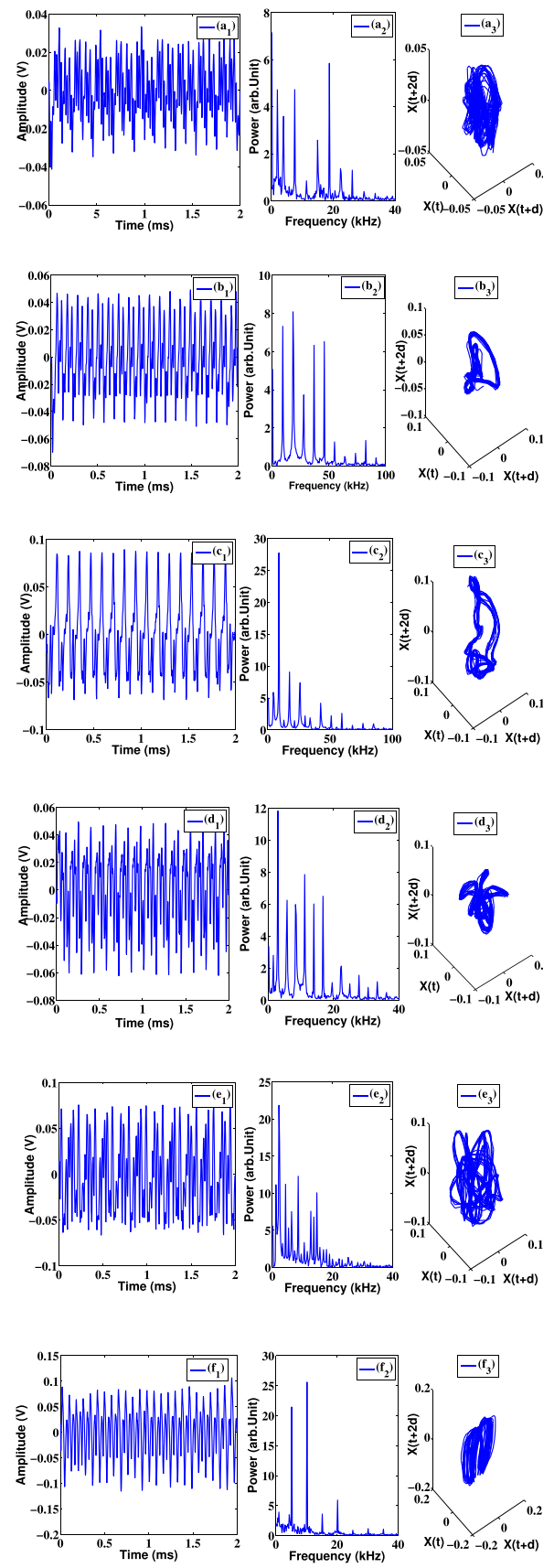
FIG. 3. (a$_1$)–(f$_1$) time series of floating potential fluctuations (V_f) at different values of discharge voltages: (a) 435 V, (b) 445 V, (c) 473 V, (d) 501 V, (e) 545 V, and (f) 597 V in 28 G magnetic field; (a$_2$)–(f$_2$) different values of power spectra of the corresponding signal; (a$_3$)–(f$_3$) 3D reconstructed states space of V_f for the same values of discharge voltages.
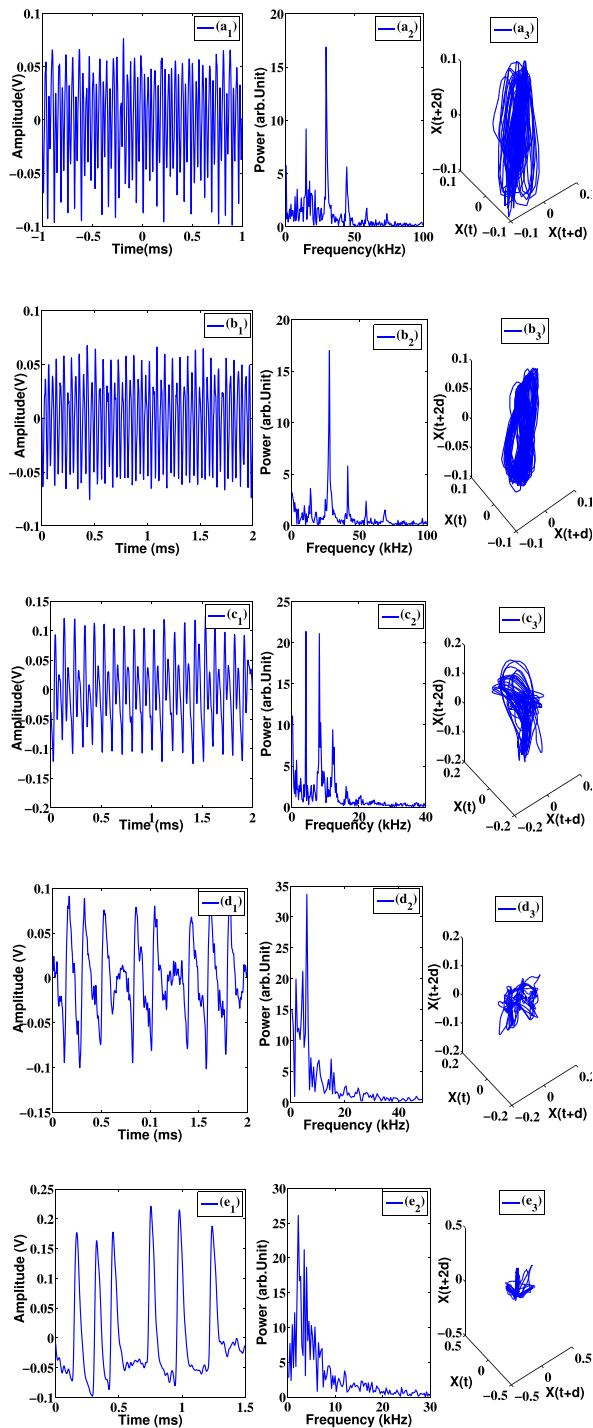
FIG. 4. (a_1)–(e_1) time series of floating potential fluctuations at different values of discharge voltages: (a) 597 V, (b) 603 V, (c) 616 V, (d) 649 V, and (e) 655 V in 46 G magnetic field; (a_2)–(e_2) different values of power spectra of the corresponding signal; (a_3)–(e_3) 3D reconstructed states space of V_f for the same values of discharge voltage.

shifted towards 10 kHz. For subsequent rising of the DV, the frequency concentration range is decreased. In the 28 G magnetic field, several distinct peaks are observed ranging from 5 kHz to 65.5 kHz as seen in Figs. $3(a_2)$–$3(f_2)$. The order state is persisting with subsequent enhancement in discharge voltage. As the magnetic field is increased to 46 G, bursts of frequencies are observed with a dominant peak at 29.5 kHz which indicates chaotic oscillation (in Fig. $4(a_2)$).

The chaotic state disappears at 603 V (Fig. $4(b_2)$) and at 649 V the peak frequency shifted towards 6 kHz leading to a relaxation oscillation of increasing time period (Figs. $4(d_2)$–$4(e_2)$). In our previous work,[13] we have found that in the absence of a magnetic field the frequency range lies between 9 and 32 kHz while introducing a magnetic field to the system increases the range of frequencies of plasma oscillations.

B. State space reconstruction

State space reconstructions of the raw data of V_f are executed by using embedding technique.[34] The appropriate state space plots are reconstructed for each time series of all the floating potential fluctuation signals obtained in different magnetic fields. It has been noticed that d and τ for all the time series lie in the range of 3–5 and 4–30. State space plots of plasma oscillations are depicted in Figs. $2(a_3)$–$2(f_3)$, $3(a_3)$–$3(f_3)$ and $4(a_3)$–$4(e_3)$. In the 9 G magnetic field, discharge is struck at 408 V. Fig. $2(a_3)$ shows several loops close to each other and Figs. $2(b_3)$–$2(f_3)$ reflects variations in the loop nature that explore quasi periodic behavior of plasma oscillations. Fig. $3(a_3)$ shows complex dynamics. Figs. $3(b_3)$ and $3(c_3)$ reveal large close loops associated with small loops reflecting large and small oscillations. Figs. $3(d_3)$–$3(f_3)$ show quasi periodic behavior. Fig. $4(a_3)$ reflects chaotic oscillation and Figs. $4(d_3)$–$4(f_3)$ relaxation oscillations via quasi periodicity. It has been noticed that when the discharge is struck the oscillations in all the cases were showing a complex nature which slightly decrease with the increase in discharge voltage.

C. RQA of plasma oscillations

Figs. 5–7 are depicting recurrence plots of floating potential fluctuations for different discharge voltages and magnetic fields. The data length considered for the RP is thousand. The threshold value has been selected in such a way that the point density was approximately 1%.[36] The changes in the character of the time series are clearly reflecting different regimes of dynamics of the plasma oscillations. Fig. 5(a) represents many small diagonal lines which are discontinuous by nature. It reflects that it might have periodicity but over laid by some low frequency variation which is visible by the low frequency oscillations present in the FFT plot. Figs. 5(b)–5(d) show long noninterrupted diagonal lines and the distance between the diagonal lines increases which indicate that in 423 V–558 V the periodicity is increasing. At 569 V, the vertical distance between the diagonal lines decreases (Fig. 5(f)) which indicates that frequencies of plasma oscillations have increased. From the distribution of the diagonal lines in the RP, it is discerned that with the increase in discharge voltages the plasma oscillation is becoming a mixed oscillation in the presence of the 9 G magnetic field, resulting in interrupted diagonal lines (Fig. 6(a)). The distance between the diagonal lines is changing under the variation of discharge voltages, indicating that the frequency of the oscillation is changing with varying discharge voltages. The long diagonal line structures found in Figs. 6(b)–6(f) indicate the periodic oscillations. Figs.
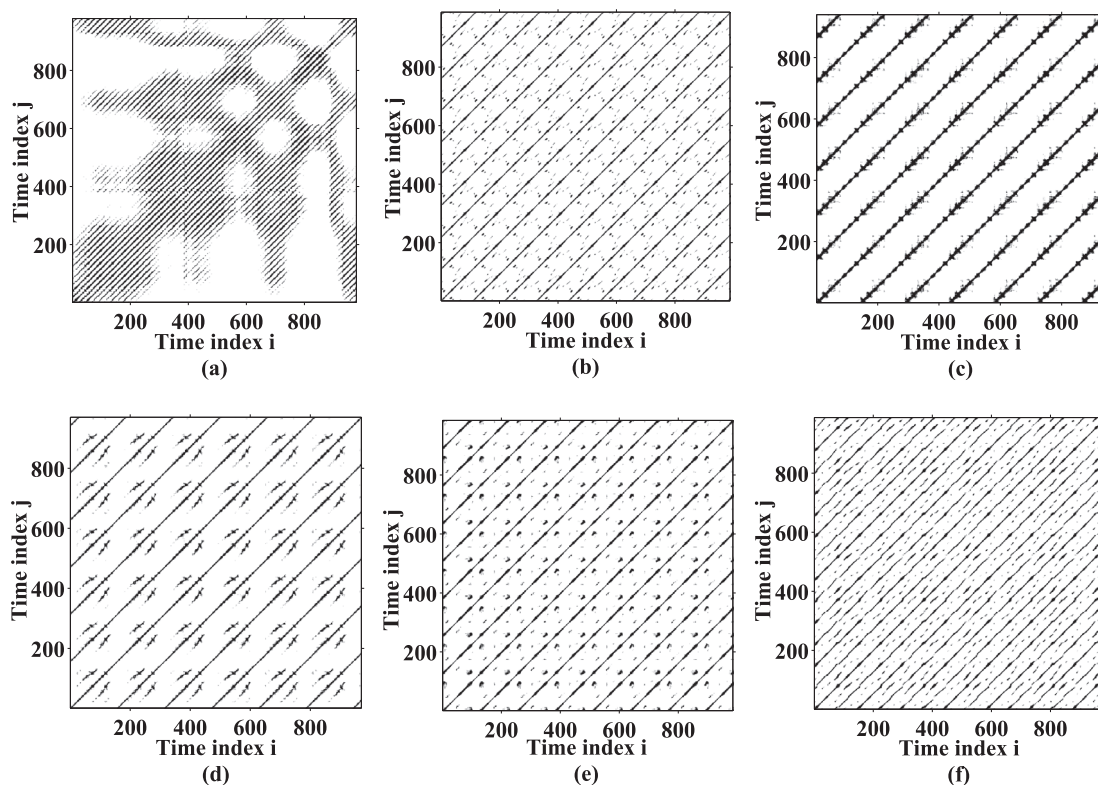
FIG. 5. Recurrence plots of the floating potential fluctuations at different discharge voltages: (a) 408 V, (b) 423 V, (c) 471 V, (d) 499 V, (e) 558 V, and (f) 569 V in the presence of 9 G magnetic field.
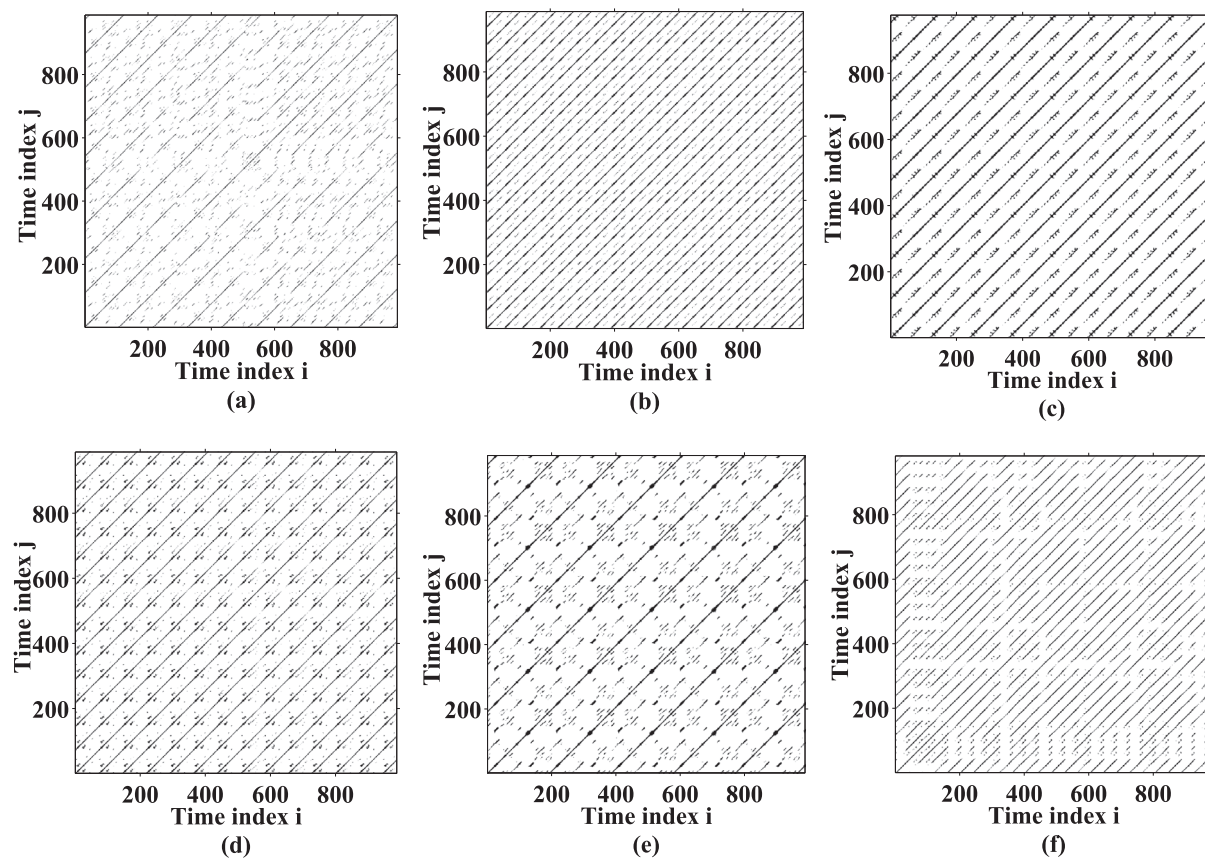

FIG. 6. Recurrence plots of the floating potential fluctuations at different discharge voltages: (a) 435 V, (b) 445 V, (c) 473 V, (d) 501 V, (e) 545 V, and (f) 597 V in the presence of 28 G magnetic field.
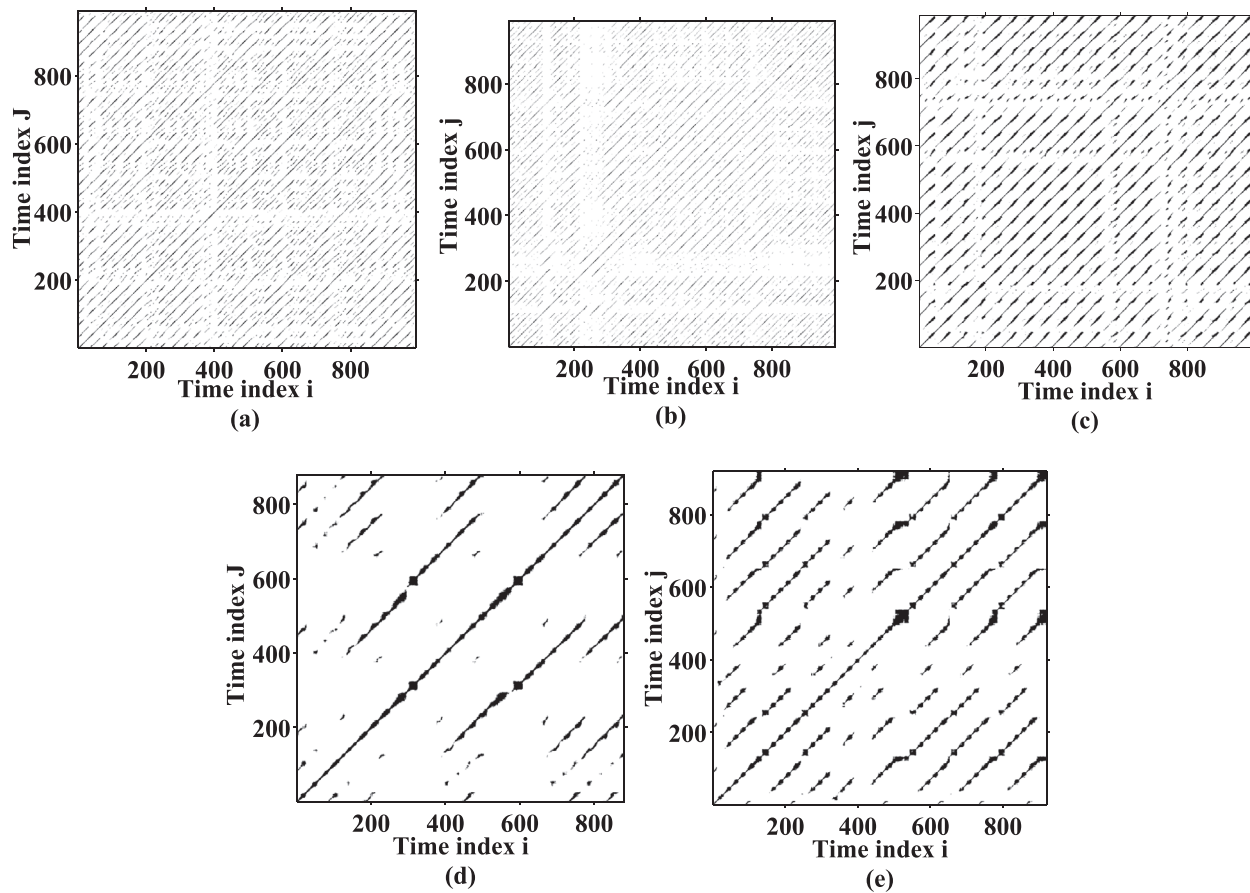
FIG. 7. Recurrence plots of the floating potential fluctuations at different discharge voltages: (a) 597 V, (b) 603 V, (c) 616 V, (d) 649 V, and (e) 655 V in the presence of 46 G magnetic field.

7(a)–7(e) show the recurrence plot of the floating potential fluctuations at 46 G magnetic field. Fig. 7(a) clearly shows short discontinuous diagonal lines which suggest that the plasma oscillation is chaotic by nature for this set of control parameters. It has been noticed that at 649 V and 655 V, the diagonal lines are short and discontinuous and the vertical distance between the diagonal lines in the RP is increased enough compared to the other plots and it is reflecting the relaxation oscillation regime.

The recurrence quantification measures determinism (*DET*), L_{max} and entropy (*ENT*) are computed for our experimental results and plotted with respect to discharge voltages. Figs. 8, 9, and 10 reflects the RQA measures for the 9 G, 28

G, and 46 G magnetic field for different discharge voltages. In this work, we are studying the dynamics as well as the statistical property of the plasma fluctuations obtained when the external magnetic field is gradually increased from 9 G to 46 G. In the 9 G magnetic field, it has been noticed that the trend of the *DET*, L_{max}, and *ENT* measures show almost an increasing trend. *DET* determines whether a signal is periodic or not. *DET* is 1 for a purely periodic signal. For the experimental time series, *DET* for a periodic signal is close to 1 (0.95) due to the influence of noise. It has been observed that with the increase in discharge voltages the value of *DET* is increasing which discern that the system is becoming more deterministic at higher discharge voltage. But the reverse
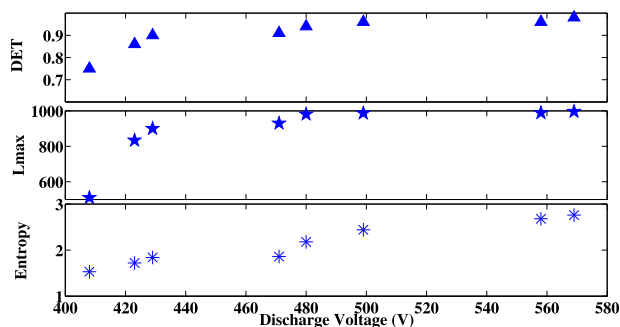

FIG. 8. Variations of recurrence quantification variables *DET*, L_{max}, and *Entropy* at different discharge voltages in 9 G magnetic field.
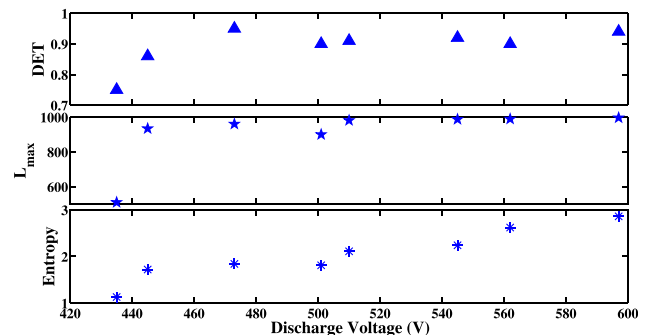

FIG. 9. Variations of recurrence quantification variables *DET*, L_{max}, and *Entropy* at different discharge voltages in 28 G magnetic field.
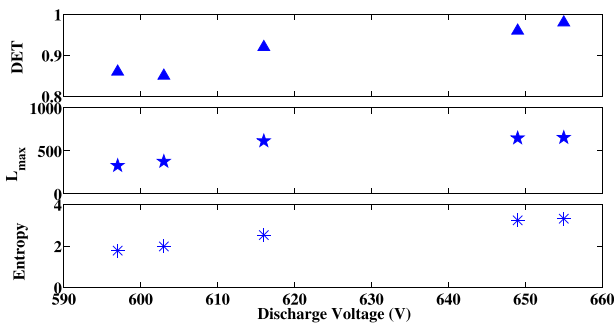
FIG. 10. Variations of recurrence quantification variables *DET*, L_{max}, and *Entropy* at different discharge voltages in 46 G magnetic field.

FIG. 12. Time series of floating potential fluctuation at 597 V in 46 G magnetic field with average and $\pm$RMS values.

phenomena are observed when the magnetic field is increased from 28 G to 46 G at 597 V. It has been noticed that with the increase of the magnetic field the value of L_{max} is decreasing. The L_{max} is minimum at 597 V in presence of 46 G magnetic field which suggests that the dynamics of the oscillation is low dimensional chaos. The Lyapunov exponent of the signal is also computed[37] by using the TISEAN Package.[38] The Lyapunov exponent for this control parameter setting is positive (0.1324) which supports the above analysis. *ENT* illustrates the complexity of the system through the statistics of the diagonal lines lengths in the RP. *ENT* is maximal if all diagonal lines are observed and attains a minimum if no or only very few diagonal lines are present (like in random or chaotic signals). In the present experiments, *ENT* values start at a low value for the chaotic signals shown in Figs. 2(a$_1$), 3(a$_1$) and 4(a$_1$) and tend to higher values for less chaotic signals with increase in DV. This is also reflected in the RPs by the changes in the diversity of the diagonal line length.[39] However, the entropic measures based on line segments are known to yield counter intuitive results when compared with the Lyapunov exponent.[15]

D. DFA of plasma oscillations

Figs. 11–14 are representing the steps of the DFA technique for the time series of floating potential fluctuations at 597 V in 46 G magnetic field. We have computed the Hurst exponent for all time series in different magnetic fields and discharge voltages for the investigation of complexity in the non-stationary time series.

Fig. 11 shows the initial step of the conversion of time series into random walk like time series.[24] The mean and
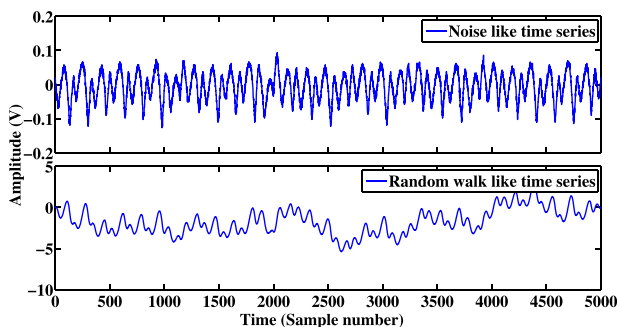

FIG. 13. The computation of local fluctuations, RMS1, around linear, quadratic, and cubic trends.

root mean square values of the time series are computed and shown in Fig. 12. The signal is divided into nonoverlapping segments of equal length and the local fluctuation functions are estimated for each segments. A polynomial trend is fitted to the data in each segment (Fig. 13). The order of the polynomial is defined by *m*. The polynomial trend is linear when $m = 1$, quadratic when $m = 2$, and cubic when $m = 3$. By averaging the local fluctuation functions for all the segments, the total fluctuation function (overall RMS) is computed.[25] The Hurst exponent (*H*) is calculated by using the power law relation between the total fluctuation functions regarding the scale. The power law relation between the overall RMS is indicated by the slope (*H*) of the regression line (Fig. 14). When *H* is in the interval of 0.5–1, the time series persists long range correlation. Moreover, *H* below 0.5 indicates anti correlation while $H = 0.5$ reflects short range dependent structures and random behaviour. Fig. 15 shows that in 9 G,

FIG. 11. Time series and Random Walk like time series of floating potential fluctuations at 597 V in 46 G magnetic field.

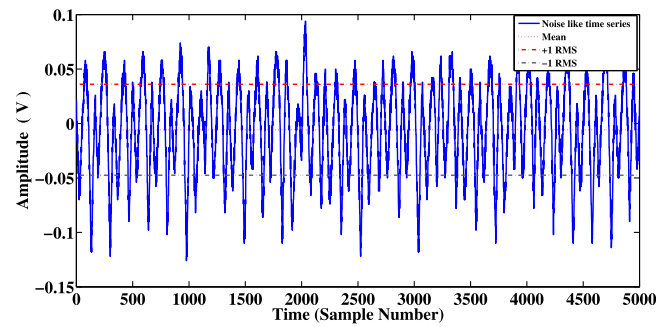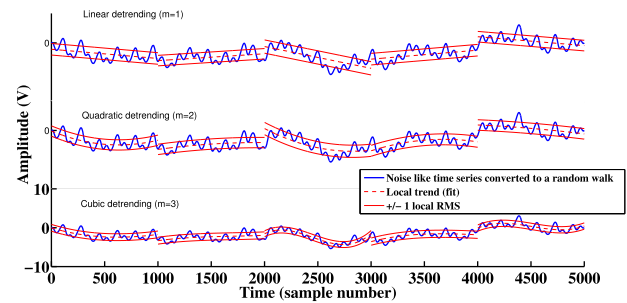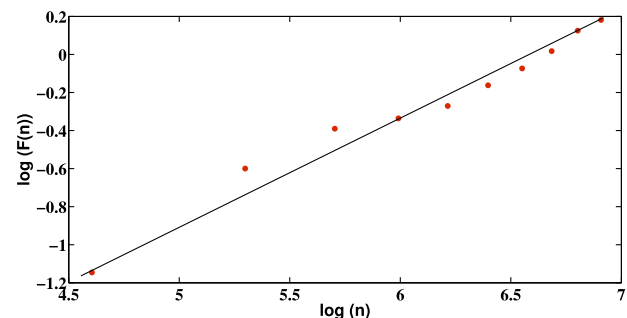FIG. 14. Plot of log(F(n)) vs log(n) for time series of floating potential fluctuation at 597 V in 46 G magnetic field.
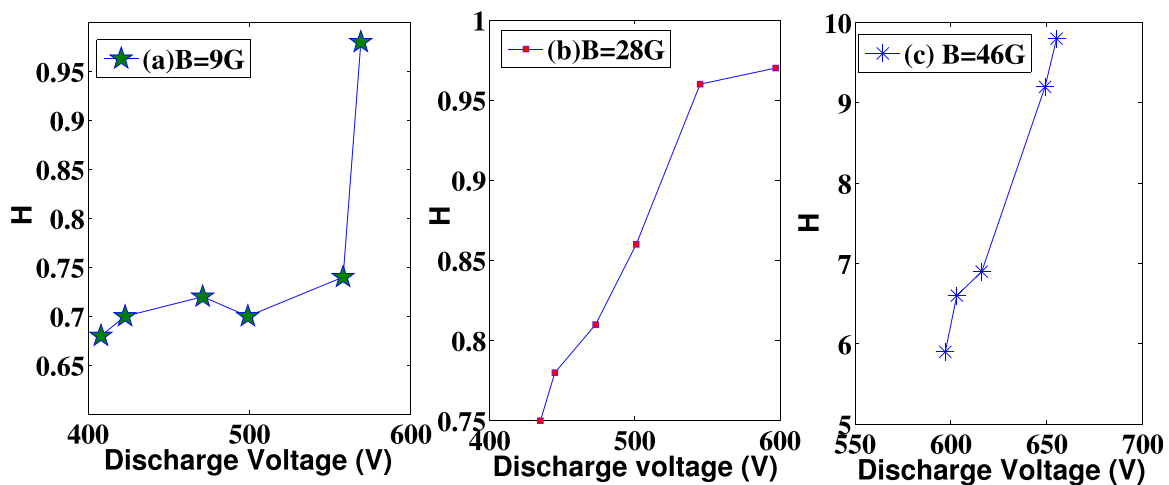
FIG. 15. Plot of Hurst exponent vs discharge voltage in different magnetic fields.

28 G, and 46 G magnetic fields, the value of the Hurst exponent of the floating potential fluctuations is increasing with the increase in discharge voltage and this elucidates that with the increase in discharge voltage long range correlation of the floating potential fluctuation grows. Hence, the oscillations are becoming regular and order with the variation of discharge voltages at a constant magnetic field. Fig. 15(a) shows the value of *H* is enhancing with the increase in discharge voltage and a sudden jump is noticed at 569 V. Figs. 15(b) and 15(c) reflect the sharp rise of *H* for the 28 G and 46 G magnetic field. Hence, Fig. 15 indicates that the complexity is decreasing with growing H. Moreover, it has been observed that in the higher magnetic field (46 G) at 597 V, the value of the *H* is approaching to 0.59. This suggests that the correlation is less and that the oscillation is more complex and irregular. Further analysis (Lyapunov exponent) also confirms that the floating potential fluctuation become chaotic at 597 V in 46 G magnetic field. Hence, the complexity of the signal is decreasing, which enhances the predictability and regularity of the data. This confirms the results of the RQA as the values of *DET* and *ENT* are also showing a similar increasing trend with the increase of discharge voltages in the respective magnetic field.

V. CONCLUSION

In this work, the three recurrence-based measures *DET*, *ENT*, and L_{max} have been used and compared with a statistical method (DFA) in order to characterize the dynamical behaviour as well as the statistical features of the glow discharge plasma oscillations in the presence of an external magnetic field. RP is an advanced technique which qualitatively and quantitatively reveals the underlying physics of the system dynamics when the system goes through a transition. The considered recurrence measures exhibit an instantaneous change which was noticed in both RPs and RQA measures. The substantial differences in the structure of diagonal lines among all the patterns displayed in the RPs clearly indicate the state transition of the plasma oscillation with the associated magnetic field. RQA diagnostics are reflecting that the dynamics of the plasma oscillation is

becoming chaotic with the increase in the magnetic field which is generating complexity in the system. A chaos to relaxation oscillation is observed with the variation of discharge voltage at a higher magnetic field (46 G). It has been found that the information retrieved from the analysis is consistent with the previous analysis carried out with conventional techniques such as the Lyapunov exponent. The scaling properties, which reflect an inner fractal structure of a time series, are alternative quantifiers of complexity in real systems. In order to comprehend the complex dynamics of the observation we have carried out DFA of plasma oscillations. It has been noticed that in a constant discharge voltage, with the increase in the magnetic field, the value of the Hurst exponent is decreasing. Hence, it elucidates the complexity of the system is increasing with the increase in the magnetic field, although the long range correlation still persists.

The main goal of the paper is to study the nonlinear features of plasma oscillations by using recurrence quantification analysis. The DFA analysis has been carried out to verify the results obtained from the RQA with the help of persistent behaviour. Both the results are indicating that the complexity is growing up in the dynamics of floating potential fluctuations with increasing magnetic field and decreasing discharge voltage. The result confirms that the recurrence-based approach is very useful because it can correctly identify the transitions between the different complex states.

This work highlights the potential of the RQA along with the DFA analysis which can be used to explore and develop the dynamical system theory of plasma oscillations of different plasma systems like DC glow discharge, double plasma, dusty plasma etc. Our analysis enriches the complexity study of the plasma instability and its associated nonlinear dynamical phenomena such as homoclinic bifurcation, mixed mode oscillation, intermittency, etc.

ACKNOWLEDGMENTS

[1]J.-P. Eckman, S. O. Kamphorst, and D. Ruelle, Europhys. Lett. **4**, 973 (1987).

[2]H. Sabelli, Nonlinear Dyn., Psychol., Life Sci. **5**, 89 (2001).

[3]T. Chelidze and T. Matcharashvili, Comput. Geosci. **29**, 587 (2003).

[4]C. Stan, C. P. Cristescu, and D. G. Dimitriu, Phys. Plasmas **17**, 042115 (2010).

[5]D. L. Toufen, Z. O. Guimarães-Filho, I. L. Caldas, J. D. Szezech, S. Lopes, R. L. Viana, and K. W. Gentlen, Phys. Plasmas **20**, 022310 (2013).

[6]O. Kopaek, V. Karas, J. Kova, and Z. Stuchlk, Astrophys. J. **722**, 1240 (2010).

[7]J. A. Hołyst and M. Zebrowska, Int. J. Theor. Appl. Finance **3**, 419 (2000).

[8]N. Marwan, M. C. Romano, M. Thiel, and J. Kurths, Phys. Rep. **438**, 237 (2007).

[9]Z. O. Guimaraes-Filho, I. L. Caldas, R. L. Vianab, J. Kurths, I. C. Nascimento, and Yu. K. Kuznetsov, Phys. Lett. A **372**, 1088 (2008).

[10]Z. O. Guimaraes-Filho, I. L. Caldas, R. L. Viana, I. C. Nascimento, Yu. K. Kuznetsov, and J. Kurths, Phys. Plasmas **17**, 012303 (2010).

[11]M. Rajkovic, T.-H. Watanabe, and M. Skoric, Phys. Plasmas **16**, 092306 (2009).

[12]J. A. Mier, R. Sanchez, L. Garcia, J. Varela, and D. E. Newman, Phys. Plasmas **18**, 062306 (2011).

[13]V. Mitra, A. Sarma, M. S. Janaki, A. N. Sekar Iyengar, B. Sarma, N. Marwan, J. Kurths, P. K. Shaw, D. Saha, and S. Ghosh, Chaos, Solitons Fractals **69**, 285 (2014).

[14]V. Mitra, B. Sarma, A. Sarma, M. S. Janaki, and A. N. Sekar Iyengar, Phys. Plasmas **23**, 032304 (2016).

[15]D. Eroglu, T. K. D. M. Peron, N. Marwan, F. A. Rodrigues, L. da, F. Costa, M. Sebek, I. Z. Kiss, and J. Kurths, Phys. Rev. E **90**, 042919 (2014).

[16]D. Weixing, H. Wie, W. Xiaodong, and C. X. Yu, Phys. Rev. Lett. **70**, 170 (1993).

[17]W. X. Ding, H. Q. She, W. Huang, and C. X. Yu, Phys. Rev. Lett. **72**, 96 (1994).

[18]M. A. Hassouba, H. I. Al-Naggar, N. M. Al-Naggar, and C. Wilke, Phys. Plasmas **13**, 073504 (2006).

[19]P. Y. Cheung and A. Y. Wong, Phys. Rev. Lett. **59**, 551 (1987).

[20]T. Braun, J. A. Lisboa, R. E. Francke, and J. A. C. Gallas, Phys. Rev. Lett. **59**, 613 (1987).

[21]A. Atipo, G. Bonhomme, and T. Pierre, Eur. Phys. J. D **19**, 79 (2002).

[22]J. Qin, L. Wang, D. P. Yuan, P. Gao, and B. Z. Zang, Phys. Rev. Lett. **63**, 163 (1989).

[23]M. Nurujjaman, R. Narayanan, and A. N. Sekar Iyengar, Chaos **17**, 043121 (2007).

[24]E. A. F. Ihelen, Front. Phys. **3**, 141 (2012).

[25]J. W. Kantrlhaldt, S. A. Zschiegner, E. K. Buunde, S. Havlin, and H. E. Stanley, Phys. A **316**, 87 (2002).

[26]F. Takens, *Lecture Notes in Mathematics* (Springer, 1981), Vol. 898, p. 366.

[27]A. M. Fraser and H. L. Swinney, Phys. Rev. A **33**, 1134 (1986).

[28]S. Schinkel, N. Marwan, O. Dimigen, and J. Kurths, Phys. Lett. A **373**, 2245 (2009).

[29]N. Marwan and J. Kurths, Phys. Lett. A. **336**, 349 (2005).

[30]C. L. Webber and J. P. Zbilut, "Recurrence quantification analysis of nonlinear dynamical systems," in *Tutorials in Contemporary Nonlinear Methods for the Behavioral Sciences*, edited by M. A. Riley and G. C. Van Orden (National Science Foundation, 2005) pp. 26–96.

[31]N. Marwan and J. Kurths, Phys. Lett. A **302**, 299 (2002).

[32]N. Marwan, Eur. Phys. J. Special Top. **164**, 3 (2008).

[33]B. Sarma, S. Chauhan, A. M. Whartan, and A. N. Sekar Iyengar, J. Plasma Phys. **79**, 885 (2013).

[34]R. Mane, "On the dimension of the compact invariant sets of certain nonlinear maps," *Dynamical systems and turbulence (Lecture Notes in Mathematics)* (Springer-Verlag, Berlin, 1981), Vol. 898, p. 230.

[35]M. B. Kennel, R. Brown, and H. D. I. Abarbanel, Phys. Rev. A **45**, 3403 (1992).

[36]M. Thiel, M. C. Romano, J. Kurths, R. Meucci, E. Allaria, and F. T. Arecchi, Phys. D **171**, 138 (2002).

[37]B. Sarma, S. S. Chauhan, A. M. Whartan, and A. N. Sekar Iyengar, Phys. Scr. **88**, 065005 (2013).

[38]R. Hegger, H. Kantz, and T. Schreiber, Chaos **9**, 413 (1999).

[39]L. L. Trulla, A. Giuliani, J. P. Zbilut, and C. L. Webber, Phys. Lett. A **223**, 255 (1996).

[40]S. V. Buldyrev, A. L. Goldberger, S. Havlin, R. N. Mantegna, M. E. Matsa, C.-K. Peng, M. Simons, and H. E. Stanley, Phys. Rev. E **51**, 5084 (1995).

[41]C.-K. Peng, S. V. Buldyrev, A. L. Goldberger, R. N. Mantegna, M. Simons, and H. E. Stanley, Phys. A **221**, 180 (1995).

[42]S. V. Buldyrev, N. V. Dokholyan, A. L. Goldberger, S. Havlin, C.-K. Peng, H. E. Stanley, and G. M. Viswanathan, Phys. A **249**, 430 (1998).

[43]C.-K. Peng, J. Mietus, J. M. Hausdorff, S. Havlin, H. E. Stanley, and A. L. Goldberger, Phys. Rev. Lett. **70**, 1343 (1993).

[44]C.-K. Peng, S. Havlin, H. E. Stanley, and A. L. Goldberger, Chaos **5**, 82 (1995).

[45]Y. H. Liu, P. Cizeau, M. Meyer, C.-K. Peng, and H. E. Stanley, Phys. A **245**, 437 (1997).

[46]M. Ausloos and K. Ivanova, Phys. A **286**, 353 (2000).

[47]E. Koscielny-Bunde, A. Bunde, S. Havlin, H. E. Roman, Y. Goldreich, and H.-J. Schellnhuber, Phys. Rev. Lett. **81**, 729 (1998).

[48]P. Talkner and R. O. Weber, Phys. Rev. E **62**, 150 (2000).

[49]J. W. Kantelhardt, R. Berkovits, S. Havlin, and A. Bunde, Phys. A **266**, 461 (1999).

[50]N. Vandewalle, M. Ausloos, M. Houssa, P. W. Mertens, and M. M. Heyns, Appl. Phys. Lett. **74**, 1579 (1999).